

Partially Cooperative Phase Conversions and Noninteger Avrami Exponents

Zhenhuan Sun, Grace G. D. Han, and Klaus Schmidt-Rohr*



Cite This: *J. Phys. Chem. C* 2024, 128, 20765–20773

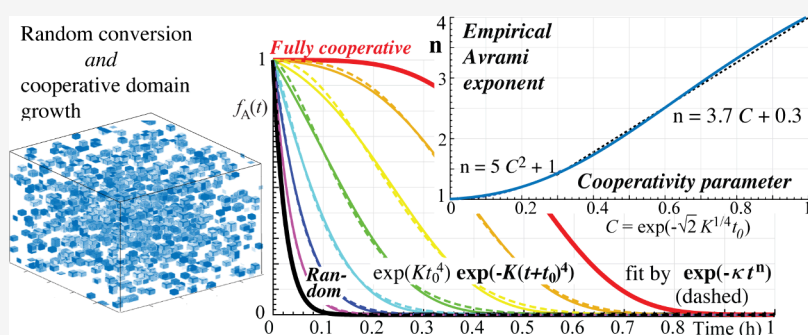


Read Online

ACCESS |

Metrics & More

Article Recommendations



ABSTRACT: Partially cooperative phase transformations, with characteristically sigmoidal conversion curves, are commonly observed, but rigorous analytical solutions are widely familiar only for fully cooperative and fully noncooperative conversions ($\exp(-Kt^4)$ and $\exp(-kt)$, respectively, in three dimensions). The JMAK formula, $\exp(-\kappa t^n)$ with noninteger Avrami exponent n , has been used to fit data for partially cooperative conversions, but this approach has only been empirical and so far seems to lack theoretical derivation and support. We show that the Ishibashi–Takagi modification of Avrami theory rigorously accounts for partial cooperativity that arises from the competition between random volume filling by newly formed nuclei of finite volume and cooperative domain growth. The imperfect cooperativity and finite initial domain volume are accounted for by a prenucleation growth time t_0 , resulting in conversion curves of the form $\exp(Kt_0^4) \exp(-K(t+t_0)^4)$, with K depending on nucleation and growth rates as in fully cooperative Avrami theory. The validity of the analytical theory, which solves the Finke–Watzky problem of competing nucleation and growth and can be cast in terms of two rate constants, has been confirmed by numerical simulations of domain growth with finite initial domain volume on a lattice with the nucleation rate varying over nearly 5 orders of magnitude. The first-order kinetics exponential decrease in the limit of no cooperativity is correctly recovered for large t_0 . Between the random and fully cooperative limits, the partially cooperative conversion curves resemble, but are not exactly matched by, empirical Avrami $\exp(-\kappa t^n)$ with a noninteger exponent or Finke–Watzky curves. A cooperativity parameter $C = \exp(-(4K)^{1/4}t_0)$ ranging between 0 and 100% is introduced and related to the empirical Avrami exponent.

1. INTRODUCTION

Many solid-state reactions and phase transformations in materials science, including photochemical^{1,2} or thermally driven^{3–5} solid-state cycloaddition of monomers and crystallization of polymers,⁶ show characteristically sigmoidal conversion curves with time. The recent observation of sigmoidal cycloreversion of a dianthracene-based molecular solar thermal (MOST) energy storage material by solid-state NMR⁷ stimulated our own interest in this phenomenon. Since random conversion results in first-order kinetics with a simple exponential decrease of the initial phase (reactant), it is clear that the sigmoidal behavior must be due to cooperative or autocatalytic processes. Conversion is fully cooperative if a volume element can convert only in contact with an already converted volume or a fresh nucleus of negligible volume. It can be modeled and described analytically in terms of domain

growth by the Avrami or Johnson–Mehl–Avrami–Kolmogorov (JMAK) theory.^{8–12} In three spatial dimensions, the case relevant here, the JMAK theory gives the time dependence of the remaining volume fraction of the initial phase ‘A’ as

$$V_A(t)/V_A(0) = \exp(-Kt^4) \quad (1)$$

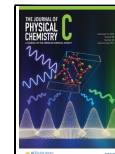
where the constant K depends on the nucleation rate density and the domain growth rate (see details below).^{12–14} The

Received: August 26, 2024

Revised: November 13, 2024

Accepted: November 14, 2024

Published: November 27, 2024



derivation of the Avrami equation has proved challenging to textbook authors^{15–17} due to the impingement of growing domains or simultaneous nucleation and growth of different domains¹⁸ but it has been presented convincingly in several sources.^{12–14}

Standard Avrami theory always implies a fully cooperative scenario and does not include a description of partial cooperativity, where volume is filled by random noncooperative conversion and cooperative domain growth in competition. While a generalized Avrami formula, $\exp(-\kappa t^n)$, has been used to interpolate between noncooperative kinetics with $\exp(-kt)$, and the fully cooperative standard Avrami eq 1, the use of noninteger exponents n has not been supported by a rigorous theory. Our analysis here documents that the equation $\exp(-\kappa t^n)$ may serve only as an approximation for partially cooperative transformations.

Herein, we analyze partially cooperative phase transformations based on Avrami theory modified to include an initial volume of the nucleus, following the pioneering work of Ishibashi and Takagi,¹³ which was based on Kolmogorov's rigorous derivation¹² of the original JMAK equation. When the size of the nucleus is finite, noncooperative filling of space by the formation of new nuclei competes with cooperative domain growth of standard Avrami theory. This corresponds to the situation of simultaneous nucleation and growth that Finke and Watzky¹⁹ sought to describe approximately by simple two-step kinetics with random nucleation $A \rightarrow B$ and cooperative growth $A + B \rightarrow 2B$.^{19,20} Our analytical theory, which exactly solves the Finke–Watzky nucleation and growth problem in a three-dimensional solid, is validated by numerical simulations of the growth of compact, convex domains with finite initial domain volume on a lattice with periodic boundary conditions, and partial filling of lattice volume elements to better model the continuous growth. The conversion curves are compared with Finke–Watzky and empirical Avrami fits. In the limit of no cooperativity, from our general formula we recover the exponential decrease due to first-order kinetics. A cooperativity parameter is introduced and related to the empirical Avrami exponent. The analytical result is also re-expressed in terms of two rate constants.

2. METHODS

2.1. Lattice Simulations of Domain Growth. Simulations were performed using MATLAB on matrices of size $240 \times 240 \times 240$, corresponding to a three-dimensional lattice of $(30 \text{ nm})^3$ in space. Matrix entries ranged between 0 and 1, representing the extent of conversion of that volume element, starting with 0 everywhere. After each time step of 1 min, growth was calculated by adding a given small growth fraction of $v/(0.125 \text{ nm}/\text{min})$ to elements facially neighboring any element with a value of 1 but capping the resulting value at 1. Periodic boundary conditions were implemented by assigning the boundaries of the system as neighbors of their counterparts on the other end. For simplicity, numerical simulations were performed in Cartesian coordinates, which spawn rounded cubic nuclei as opposed to exactly spherical ones and may lead to nonconvex domains in the beginning of growth. This issue was mitigated by using larger nuclei of dimensions $8 \times 8 \times 8$, where concavity is negligible. Fractional filling of volume elements allows growth to be much finer grained, making it unnecessary to scale up the system size excessively.

Nucleation (with nuclei of size $V_0 = 8 \times 8 \times 8 = 1 \text{ nm}^3$) was simulated by generating a $30 \times 30 \times 30$ random matrix and

then scaling it up to $240 \times 240 \times 240$ lattice elements; a value of 1 was assigned to all volume elements whose corresponding random value was smaller than that of the small input nucleation probability of $n \text{ nm}^3 \text{ min}$. A total of 800 time steps of 1 min each were calculated. All simulations were repeated 32 times and averaged to reduce random noise from the nucleation step.

3. BACKGROUND

3.1. Random Noncooperative Conversion of A to B. An important limiting case in phase transformation is uncorrelated or random conversion of A to B. Each volume element has a certain probability of converting within a given time period, independent of its neighbors. In this case, phase conversion exhibits first-order kinetics as described by the simple proportionality $|dN_A/dt| \sim N_A(t)$, which is the number of volume elements of type A at time t . The volume still occupied by the unconverted phase at time t , $V_A(t)$, is given by

$$V_A(t) = V_0 N_A(t) \quad (2)$$

where V_0 represents the volume of one element. With the nucleation rate per volume n (i.e., the number of nuclei formed per volume and time), we can express the rate of conversion as

$$|dN_A/dt| = n V_A(t) = n V_0 N_A(t) \quad (3)$$

which gives the first-order rate law

$$dN_A/dt = -n V_0 N_A(t) = -k_1 N_A(t) \quad (4)$$

with

$$k_1 = n V_0 \quad (5)$$

The well-known solution of eq 4 is the exponential decrease of the fraction f_A of component A typical of first-order kinetics:

$$\begin{aligned} N_A(t)/N_A(0) &= V_A(t)/V_A(0) \\ &= f_A(t) = \exp(-k_1 t) = \exp(-n V_0 t) \end{aligned} \quad (6)$$

3.2. Avrami Theory: Debated Derivation. Avrami or JMAK theory^{8–12} describing the filling of space by growing domain is a fully cooperative process. In this study, interest is focused on domain growth in three dimensions from nuclei generated randomly in space and time. Progressive filling of volume by growing domains limits the space where new nuclei can form, and growing domains progressively overlap. These probabilistic effects complicate the analysis. Major challenges include how to correctly account for the already converted volume and for random nucleation. The mathematically rigorous analysis by Kolmogorov¹² has rarely been discussed, but it was notably used by Ishibashi and Takagi.¹³ The derivation by Avrami refers to perplexing “phantom nuclei” and “extended volume” concepts, which have been questioned in the literature.^{12,18}

Textbooks struggle with presenting a valid, understandable derivation of Avrami theory. Strobl¹⁵ finds it preferable not to present a proof; Sperling's¹⁶ derivation contains at least two conceptually relevant typographical errors; Young¹⁷ tells readers that “one can show that...” the equation can be derived and adds a factor of 2 to the Avrami constant in 3D; the proof presently on Wikipedia convinces at short times only. Gedde's¹⁴ proof is correct but also so brief and lacking the needed diagrams that it is difficult to follow. It is also confounding that various symbols are used for the same rates

by different authors. We review an instructive and rigorous derivation of the Avrami formula and then modify it to incorporate the finite initial volume, V_0 , of a nucleus.

3.3. Avrami Theory: A Rigorous Derivation. In the following, we review and interpolate Gedde's¹⁴ derivation of the Avrami/JMAK formula in 3D, as a basis for its subsequent modification for partially cooperative processes.

Consider a point P surrounded by a spherical shell of radius r and thickness dr as shown in Figure 1. In the spherical shell,

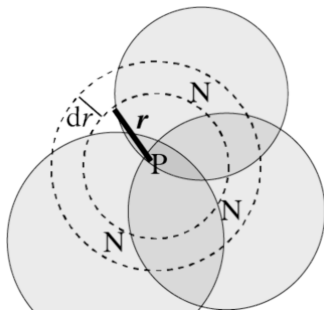


Figure 1. Representation of domains nucleated at a distance r from a generic point P in space and reaching that point at a time $t \geq r/v$.

nuclei are generated with a rate density \dot{n} (number per time and per volume) and then expand with a growth front speed v . The average number dE of growth fronts nucleated in the spherical shell that pass the point P in the center is obtained according to

$$dE = dV\dot{n}\Delta t \quad (7)$$

with the shell volume $dV = 4\pi r^2 dr$ and the time Δt during which growing domains from the shell can reach the point in the center,

$$\Delta t = t - r/v \quad (8)$$

The travel time $\tau = r/v$ between shell and center, during which no growth front reaches the center yet, is properly subtracted out from the total time t . Then

$$dE = dV\dot{n}\Delta t = 4\pi r^2 dr\dot{n}(t - r/v) \quad (9)$$

We integrate space around point P from 0 to vt , the maximum distance from which growing domains can reach the point P within time t , to obtain the average number E of growth fronts passing through the point:

$$E = \frac{4\pi\dot{n}}{v} \int_0^{vt} r^2(vt - r)dr = 12K\frac{1}{3}t^3 - 12K\frac{1}{4}t^4 = Kt^4 \quad (10)$$

with

$$K = (\pi/3)v^3\dot{n} \quad (11)$$

the well-known constant of Avrami theory in 3D with random nucleation. It is notable that the product $v^3\dot{n}$ in K combines the effects of nucleation and growth rates in such a way that they cannot be determined independently. According to Poisson theory (see next section), the probability that within time t no growth front has passed through a given point, i.e., the remaining fraction $f_A(t)$, is

$$f_A(t) = \exp(-E) = \exp(-Kt^4) \quad (12)$$

A new nucleus potentially occurring in an already converted region does not pose a problem in this analysis.

3.4. Poisson Statistics. The last step of the derivation of eq 12 refers to a result of Poisson statistics, which is reviewed in the following. For a process occurring with a constant rate λ over a time interval t , the expected number of events with the time t is

$$E = \text{rate} \times \text{time period} = \lambda t \quad (13)$$

If t is divided into N small subintervals of equal length t/N with very big N , such that only one event can occur in any subinterval, the probability of an event occurring is $\frac{\lambda t}{N}$, and of no event is $1 - \frac{\lambda t}{N}$ in each interval. The probability of exactly m events in the total time t (leaving $N - m$ intervals without events) is given by the binomial distribution:

$$P(m) = \frac{N!}{m!(N-m)!} \left(\frac{\lambda t}{N}\right)^m \left(1 - \frac{\lambda t}{N}\right)^{N-m} \quad (14)$$

where the first factor is the number of permutations of m intervals with events and $(N - m)$ intervals without. Taking the limit of $N \rightarrow \infty$, i.e., $N \gg m$, neglecting m relative to N , we find

$$\begin{aligned} & \lim_{N \rightarrow \infty} \frac{N!}{(N - m)!} \\ &= \lim_{N \rightarrow \infty} \frac{N(N-1)\cdots(N-m+1)(N-m)!}{(N-m)!} \\ &= N^m \end{aligned} \quad (15a)$$

$$\lim_{N \rightarrow \infty} \left(1 - \frac{\lambda t}{N}\right)^{N-m} = e^{-\lambda t} \quad (15b)$$

Inserting these two limits into the binomial distribution yields the Poisson distribution

$$P(m) = \frac{N^m}{m!} \left(\frac{\lambda t}{N}\right)^m e^{-\lambda t} = \frac{E^m}{m!} e^{-E} \quad (16)$$

which is independent of the chosen number N of intervals. The average number of events within the time t is

$$\begin{aligned} \langle m \rangle &= \sum_{m=0}^{\infty} mP(m) \\ &= 0 + \sum_{m=1}^{\infty} m \frac{E^m}{m!} e^{-E} \\ &= Ee^{-E} \sum_{m=1}^{\infty} \frac{E^{m-1}}{(m-1)!} \\ &= Ee^{-E} \sum_{m=0}^{\infty} \frac{E^{m'}}{m'!} = Ee^{-E} e^E = E \end{aligned} \quad (17)$$

consistent with eq 13.

3.5. Raindrops on a Pond. The probability of a certain number of waves passing a point on a pond with raindrops falling at a constant rate \dot{n} is a classical application of the Poisson distribution and conceptually related to Avrami theory in 2D. When a raindrop hits the surface, a circular water wave propagates out radially from the point of impact with velocity v . This is analogous to the growth of circular domains from nuclei generated randomly with constant rate \dot{n} per time and

area. The probability that exactly m waves have reached an arbitrary point (i.e., the probability of m events) within time t is given by the Poisson distribution of eq 16:

$$P(m) = \frac{E^m(t)}{m!} e^{-E(t)}$$

$E(t)$ is the average number of waves that have reached the point within time t , which can be calculated through integrating the number of raindrops that have fallen at time τ and have propagated for a period of $t - \tau$:

$$E(t) = \int_0^t \dot{n}\pi[v(t - \tau)]^2 d\tau = \frac{1}{3}\dot{n}\pi v^2 t^3 \quad (18)$$

Importantly, the probability of no waves having reached the point within time t is, according to eq 16, given by

$$P(0) = e^{-E(t)} = e^{-\kappa t^3} \quad \text{with } \kappa = \frac{1}{3}\dot{n}\pi v^2 \quad (19)$$

which is the Avrami equation in 2D. In three dimensions, the propagation, as shown in Figure 1, is out of a spherical shell instead of a circle, resulting in eq 10.

3.6. Avrami Theory with Partial Cooperativity: The Finke–Watzky Problem. In contrast to the fully cooperative process described by standard Avrami theory, where growth starts solely in contact with existing nuclei (defined as points of zero volume), we propose a partially cooperative model. In this model, randomly generated nuclei of finite size are introduced into the system and fill volume alongside domain growth. The cooperative conversion resulting from contact with existing phases competes with that resulting from randomly generated nuclei. This is the problem of competing nucleation and growth posed in 1997 by Finke and Watzky,¹⁹ which we solve here in three spatial dimensions instead of using simplifying kinetics equations.

This model can be implemented by a modification of 3D Avrami theory. In Avrami theory, a nucleus is “born” as a point of zero volume (Figure 2a), so without growth, volume will not

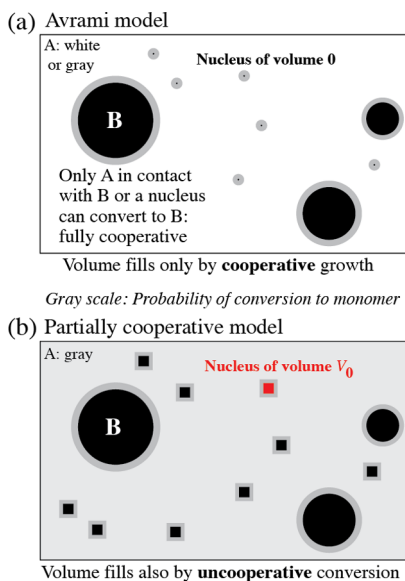


Figure 2. Cartoons comparing (a) the conventional Avrami model, with vanishing initial volume of a nucleus, and (b) the Ishibashi–Takagi model with nuclei of initial volume V_0 . Grayscale indicates the probability of conversion to monomer in the next time step.

be filled by the new phase. In contrast, in our partially cooperative model, see Figure 2b, a nucleus initiates with a finite volume V_0 for instance representing the volume of a lattice element. This departure from the zero-volume initiation in Avrami theory reflects the real-world scenario where domains have a finite size from the beginning. Ishibashi and Takagi¹³ introduced and solved this model, but without reference to cooperativity, by applying an advanced mathematical method introduced by Kolmogorov.¹² Here, we present an instructive derivation of the resulting equation in the context of cooperativity, elucidating how partial cooperativity influences the kinetics of phase transformations.

3.7. Avrami Theory Modified with Prenucleation

Growth Time. The initial volume (or “volume at birth”) V_0 of a nucleus is the volume of one lattice element. It can be incorporated¹³ into Avrami theory by assuming that every domain started growing to the volume V_0 during a “prenucleation growth time” t_0 , even before the nucleus formed. The initial radius

$$r_0 = vt_0 \quad (20)$$

with prenucleation growth time t_0 and linear growth velocity v (e.g., in nm/min) relates to the initial volume V_0 as expected:

$$V_0 = (4/3)\pi r_0^3 = (4/3)\pi v^3 t_0^3 \quad (21)$$

Now we calculate again, as in eq 7, the average number dE of growth fronts passing a central point P having started from nuclei in a surrounding spherical shell of radius r , see Figure 3, but the time Δt during which growing domains from the spherical shell can reach the point in the center is modified to

$$\Delta t = t - (r/v - t_0) \quad (22)$$

or

$$\Delta t = t - (r - r_0)/v \quad (23)$$

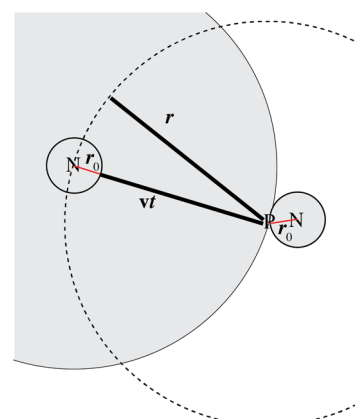


Figure 3. Representation of (left side) a domain nucleated at a distance r from a generic point P in space and reaching that point at a time $t = (r - r_0)/v$. Right side: a nucleus touching the point P at time 0 is centered at a distance r_0 from the point.

The travel time $\tau = (r/v - t_0)$ between shell and center, during which no growth fronts can reach the center yet, is reduced by the “head start” due to the prenucleation growth time t_0 . Then

$$dE = dV \dot{n} \Delta t = 4\pi r^2 dr (t - (r/v - t_0)) \quad (24)$$

We integrate space around point P from $r = r_0 = vt_0$, the closest approach between P and another nucleus, to $r = vt + r_0$, the furthest distance of a nucleus from which a growth front could reach point P, see Figure 3, to obtain the average number E of fronts passing through point P within the time t :

$$\begin{aligned}
 E &= \frac{4\pi\dot{n}}{v} \int_{r_0}^{vt+r_0} r^2(vt + vt_0 - r)dr + E_0 \\
 &= \frac{4\pi\dot{n}}{v} \left[\int_{r_0}^{vt+vt_0} r^2(vt + vt_0)dr - \int_{r_0}^{vt+vt_0} r^3 dr \right] + V_0\dot{n}t \\
 &= \frac{4\pi\dot{n}}{v} \left\{ \frac{1}{3}[(vt + vt_0)^4 - r_0^3(vt + vt_0)] - \frac{1}{4}[(vt + vt_0)^4 \right. \\
 &\quad \left. - vt_0^4] \right\} + \frac{4}{3}\pi v^3 t_0^3 \dot{n}t \\
 &= \frac{4\pi\dot{n}}{v} \left(-\frac{1}{3}v^4 t_0^3 t \right) + K(t + t_0)^4 - Kt_0^4 + 4Kt_0^3 t \\
 &= K(t + t_0)^4 - Kt_0^4
 \end{aligned} \quad (25)$$

Through the term E_0 , the probability of a new domain arising within V_0 has been taken into account. The number of growth fronts it adds is

$$E_0 = V_0\dot{n}t = 4/3\pi v^3 t_0^3 \dot{n}t = 4Kt_0^3 t \quad (26)$$

From the average in eq 25 we calculate as before the probability that no growth front has passed through a given point, i.e., the remaining fraction $f_A(t)$:

$$f_A(t) = \exp(-E) = \exp(Kt_0^4) \exp(-K(t + t_0)^4) \quad (27)$$

with $K = (\pi/3)v^3\dot{n}$. This is the same constant as in fully cooperative Avrami theory, eqs 11 and 12, which is the limit of eq 27 for $t_0 = 0$ (i.e., with zero initial volume of a nucleus). In terms of the underlying physical parameters of nucleation rate \dot{n} , speed v of a growth front, and initial radius r_0 of the nucleus when formed, eq 27 can be written as

$$f_A(t) = \exp((\pi/3)\dot{n}r_0^4/v(1 - (1 + tv/r_0)^4)) \quad (28)$$

where we have used eqs 11 and 20.

4. RESULTS AND DISCUSSION

4.1. Validation by Numerical Simulations of Compact Convex Domain Growth. In the following, we validate the abstract analytical theory with numerical simulations on a lattice with varying nucleation and growth rates, as visualized in Figure 4 for low, intermediate, and high degree of cooperativity. Figure 5a shows conversion curves generated from a series of such numerical simulations where $K \sim v^3\dot{n}$ of eq 11 was held nearly constant through simultaneous scaling of the nucleation rate \dot{n} by x and the growth rate v by $x^{-1/3}$. In the simulations, \dot{n} was varied over 4.5 orders of magnitude. In order to account for the change in particle shape recognized in Figure 4c, the effective growth rate v_{eff} was determined from the volume of a single growing domain, $V = 4\pi/3(v_{\text{eff}}(t + t_0))^3$, for the last third of the growth period, resulting in $\leq 15\%$ corrections of v_{eff} relative to microscopic v (see the legend in Figure 5a). The curves from the simulation were fitted with the analytical eq eq 27. With K nearly constant, t_0 was the dominant fit parameter in eq 27. Given that the lattice element volume V_0 and spacing r_0 were implicitly fixed, based on eq 20 we obtain the proportionality $t_0 = r_0(1/v)$, which is confirmed

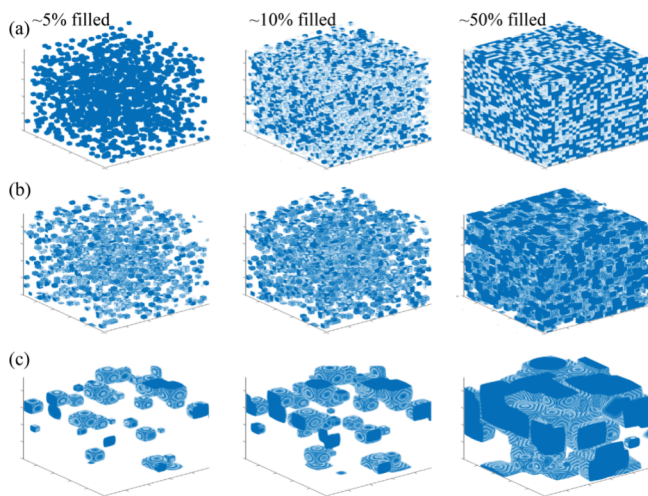


Figure 4. Snapshots of simulations of phase conversion that is (a) nearly random, with $v = 0.625 \times 10^{-3}$ nm/min and $\dot{n} = 5 \times 10^{-2}$ /nm 3 /min; (b) partially cooperative, with larger growth-front speed $v = 3.1 \times 10^{-3}$ nm/min and smaller nucleation rate $\dot{n} = 4 \times 10^{-4}$ /nm 3 /min; (c) nearly fully cooperative, with $v = 12.5 \times 10^{-3}$ nm/min and very small $\dot{n} = 6.25 \times 10^{-6}$ /nm 3 /min. To different degrees, noncooperative nucleation of new domains of finite initial volume competes with cooperative growth of existing ones. Box size: (30 nm) 3 . Shading reflects incomplete filling of a volume element of the lattice near the surface of a growing domain.

by the predicted linear increase in t_0 with the inverse of the effective growth rate in Figure 5b.

4.2. Partially Cooperative Conversion vs Empirical Generalized Avrami Formula. Figure 6 compares rigorous partially cooperative $f_A(t) = \exp(Kt_0^4) \exp(-K(t + t_0)^4)$ where $K = (\pi/3)v^3\dot{n}$ was fixed at $K = 10/h^4$ while $t_0 = v/r_0$ was varied widely, with fits based on the empirically generalized Avrami formula $f_A(t) = \exp(-\kappa t^n)$ (dashed), where both κ and n were adjusted as fitting parameters. The empirical Avrami formula shows the predicted behavior of decreasing Avrami exponent n approaching 1 as t_0 increases but fails to provide precise fits in the intermediate partially cooperative cases (note the deviation between solid curves and dashed fits). This comparison documents that the noninteger Avrami formula is just an approximation to our rigorously derived partially cooperative nucleation-and-growth model. As fit functions, both formulas give fairly similar curves with varying sigmoidal character.

4.3. Vanishing Cooperativity: Recovering Exponential Kinetics. In the limit of vanishing domain growth rate $v \rightarrow 0$, while keeping the volume of the lattice element V_0 and its radius r_0 constant, volume is filled by nongrowing domains, randomly placed. In this limit we expect eq 27 to recover simple first-order kinetics as in eq 6. This is confirmed mathematically in the following.

Using constant $r_0 = vt_0$ from eq 20 and Taylor expansion of the second exponent in eq 27, with

$$t/t_0 = vt/r_0 \ll 1 \quad (29)$$

which is small due to its proportionality to $v \rightarrow 0$, we can write

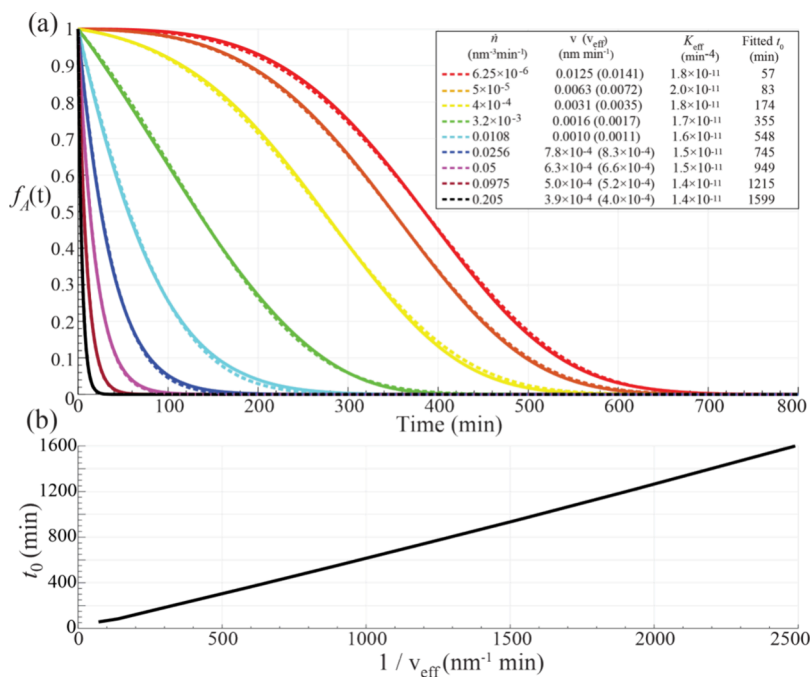


Figure 5. (a) Comparison of partially cooperative conversion obtained from numerical modeling as shown in Figure 4 (solid curves) with the analytical eq 27 (dashed curves), using the parameters shown in the legend, with the nucleation rate \dot{n} varying by 4.5 orders of magnitude. Small deviations between the accurate analytical curves for spherical particles and the simulations on a cubic lattice arise from differences in particle shape, see also Figure 4. (b) Prenucleation growth time t_0 as a function of the inverse of the effective growth rate v_{eff} (with the constant effective radius $r_0 = 0.62$ nm of a lattice element as the proportionality constant according to eq 20) from the fits in (a).

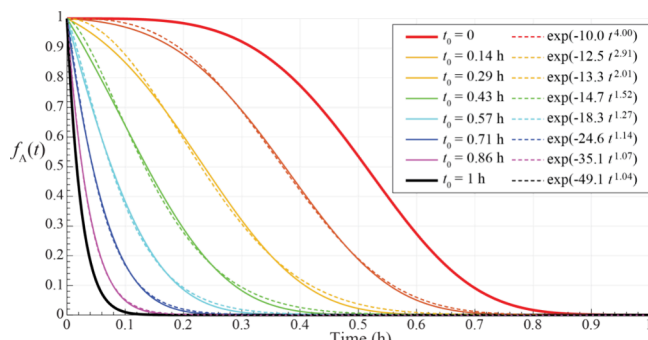


Figure 6. Comparison of (solid lines) partially cooperative conversion $f_A(t) = \exp(-Kt_0^4) \exp(-K(t + t_0)^4)$, for the t_0 values given in the legend and $K = (\pi/3)v^3\dot{n} = 10/h^4$ held fixed, with (dashed) best fits by the empirically generalized Avrami formula $f_A(t) = \exp(-kt^{\kappa})$, where both n and κ are free fit parameters without theoretical underpinnings.

$$\begin{aligned}
 f_A(t) &= \exp(Kt_0^4) \exp(-Kt_0^4(t/t_0 + 1)^4) \\
 &= \exp(Kt_0^4(1 - (vt/r_0 + 1)^4)) \\
 &\approx \exp(Kt_0^4(1 - (1 + 4vt/r_0))) \\
 &= \exp(-4Kt_0^4t/t_0) = \exp(-4Kt_0^3t)
 \end{aligned} \tag{30}$$

Inserting $K = (\pi/3)v^3\dot{n}$ from eq 11 and using eq 21 for V_0 , we obtain

$$f_A(t) \approx \exp(-4\pi/3v^3\dot{n}t_0^3t) = \exp(-\dot{n}V_0t) = \exp(-k_1t) \tag{31}$$

with

$$k_1 = 4Kt_0^3 = 4/3\pi v^3\dot{n}t_0^3 = \dot{n}V_0 \tag{32}$$

exactly reproducing the exponential noncooperative first-order conversion of eqs 6 and 5 in this limit. Due to $t/t_0 \ll 1$, see eq 29, this slow-growth limit corresponds to large

$$t_0 \gg t \approx k_1^{-1} = 1/(\dot{n}V_0) \tag{33}$$

where the approximate equality arises from the conversion occurring on the time scale of the correlation time k_1^{-1} . The outer relation of eq 33 is confirmed by the simulated conversion curves in Figure 7, which approach the exponential shape when t_0 exceeds $1/(\dot{n}V_0) = 1/(3.2 \times 10^{-3} \text{ min}^{-1}) = 3100$ min.

4.4. Conversions at Constant Nucleation Rate and Initial Nucleus Volume. Figure 7 shows an instructive series of simulated conversion curves for constant initial volume V_0 of the nucleus and constant nucleation rate $\dot{n} = 3.2 \times 10^{-3} \text{ nm}^{-3} \text{ min}^{-1}$, with the domain growth rate v as the variable

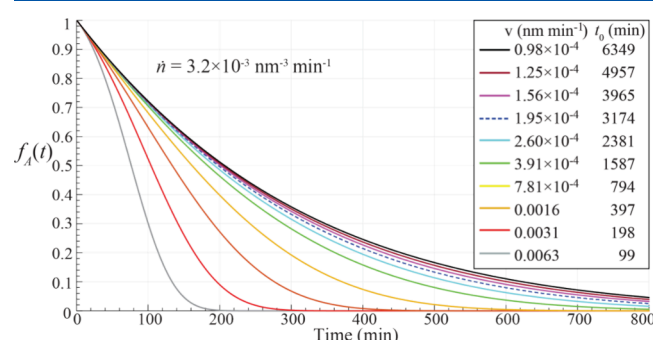


Figure 7. Series of simulated curves for constant nucleation rate $\dot{n} = 3.2 \times 10^{-3} \text{ nm}^{-3} \text{ min}^{-1}$ and constant initial nucleus volume $V_0 = 1 \text{ nm}^3$ with decreasing growth rate v , and consequently increasing $t_0 = r_0/v$, from left to right, as indicated in the legend.

parameter. At high growth rates, conversion is fast but as domain growth lags, the overall process slows down and the exponential noncooperative conversion of eqs 6 and 31 becomes the asymptotic limit. V_0 is much easier to hold fixed in lattice simulations than in the analytical expression of eq 27 given in terms of K and t_0 , but fundamentally the two approaches of course remain equivalent.

The curves of Figure 7 document that for fixed finite V_0 or equivalently r_0 , the effects of the rates \dot{n} and v can be assessed separately in

$$\exp(-K(t + t_0)^4) = \exp(-\pi/3v^3\dot{n}(t + r_0/v)^4) \quad (34)$$

while they are fundamentally inseparable as a factor $v^3\dot{n}$ in their effect on the fully cooperative Avrami behavior with $\exp(-Kt^4) = \exp(-\pi/3(v^3\dot{n})t^4)$. In some cases, with t_0 determined by fitting the curve and r_0 from the elementary volume V_0 (e.g., of a dimer in a cycloreversion process), the growth rate (or speed) $v = r_0/t_0$ could be estimated.

4.5. Physical Interpretation of V_0 , r_0 , and t_0 . The elementary volume V_0 “at birth” of a nucleus is an important parameter in the theory of partially cooperative phase conversion developed here, which extends it beyond the limitations of the original fully cooperative Avrami model. V_0 often has an intuitive meaning: it may be the volume of the critical nucleus of a crystallizing polymer chain,⁶ the volume of a disintegrating dimer in a cycloreversion process,²¹ or the volume of individual species A or B in Finke–Watzky theory (see below). In simulations it is the volume of the lattice element(s) that a nucleus occupies when it is formed. V_0 is closely related to the radius r_0 of the nucleus when first formed, via $V_0 = 4/3\pi r_0^3$.

The prenucleation growth time t_0 is introduced mainly out of notational convenience that keeps a notional link to the Avrami equation. It is the time period for which the nucleus would have had to grow from an initial point in space to reach the volume V_0 . Eq 28 shows how t_0 could be avoided in our analytical expression for the conversion curves, but at the expense of one more parameter in the expression. Comparison with the simpler eq 27 in terms of t_0 and K documents that the conversion curves depend only on two functional parameters, one of which is conveniently chosen to be t_0 .

4.6. Cooperativity Parameter. The theory presented here can correctly describe the continuum between vanishing cooperativity (exponential decrease) and full cooperativity (3D Avrami model). The degree of cooperativity can be quantified by a unitless cooperativity parameter C with values between 0 (no cooperativity) and 1 (100% cooperativity) defined as

$$C = \exp(-(k_1 t_0)^{1/4}) = \exp(-\sqrt{2} K^{1/4} t_0) \quad (35)$$

where $k_1 = 4Kt_0^3$ according to eq 31. In terms of the underlying physical parameters, based on eqs 11 and 20 we can write

$$C = \exp(-1.43(\dot{n}/v)^{1/4}r_0) \quad (36)$$

In the limits of small and large t_0 , we find

$$t_0 = 0: \quad C = \exp(-0) = 1$$

corresponding to the fully cooperative Avrami model with no volume filling from conversion of individual units ($V_0 = 0$), and

$$t_0 \rightarrow \infty: \quad C = \exp(-\infty) = 0$$

corresponding to no growth of nuclei, random volume filling, no cooperativity, and exponential decrease. With the time constant $t_{1/2}$ of decay to 50%, which for the fully cooperative Avrami model equals $t_{1/2,\text{coop}} = 0.92/K^{1/4}$, for processes with the same nucleation and growth rates (and therefore the same K) but different V_0 and therefore different degrees of cooperativity, see Figure 5, we find

$$C \approx t_{1/2}/t_{1/2,\text{coop}} \quad (37)$$

as documented in Figure 8. This provides additional justification for the exponent of 1/4 in the expression for C

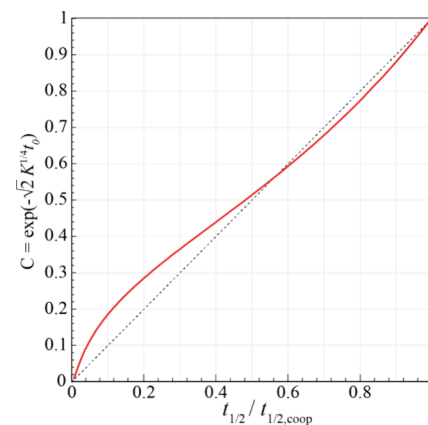


Figure 8. Correlation between normalized “half-life” $t_{1/2}$ and the cooperativity parameter $C = \exp(-\sqrt{2} K^{1/4} t_0)$. The relation is roughly linear.

in eq 35. With reduced cooperativity, noncooperative conversion speeds up the process and $t_{1/2}$ decreases, see Figure 5. In the nearly random, partially cooperative, and nearly fully cooperative simulations visualized in Figure 4a–c, the cooperativity parameters were 0.07, 0.60, and 0.85, respectively.

4.7. Cooperativity Parameter and Avrami Exponent. In the literature, the Avrami exponent n has implicitly been treated as a cooperativity parameter² but Avrami theory provides no basis for this assumption since it does not produce noninteger n that is not a multiple of $1/2$. The relation between Avrami exponent n and cooperativity parameter C , obtained by best-fitting one model with the other as in Figure 6, is shown in Figure 9.

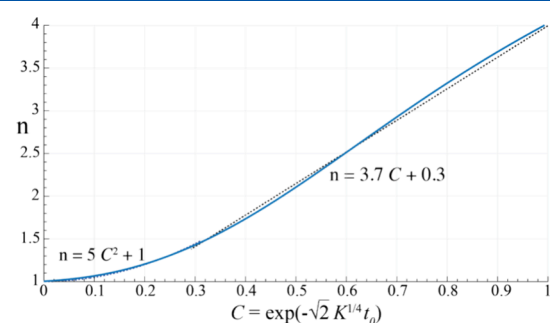


Figure 9. Correlation between the cooperativity parameter C and the empirical Avrami exponent n , obtained by best fitting as shown in Figure 5. Two simple approximations are shown as dashed curves and allow for easy conversion between n and C .

The relationship can be closely approximated, see the dashed parabola and straight line in **Figure 9**, by

$$n \approx 5C^2 + 1 \quad \text{for } C < 0.3 \quad (38a)$$

$$n \approx 3.7C + 0.3 \quad \text{for } C \geq 0.3 \quad (38b)$$

or conversely

$$C \approx \sqrt{((n - 1)/5)} \quad \text{for } n < 1.45 \quad (39a)$$

$$C \approx (n - 0.3)/3.7 \quad \text{for } n \geq 1.45 \quad (39b)$$

This plot and the simple equations make it easy to determine the cooperativity parameter C from the exponent n in a conventional empirical Avrami fit.

4.8. Comparison with Finke–Watzky Theory. The problem of competing nucleation and growth solved in this paper for the solid state was posed in 1997 by Finke and Watzky.¹⁹ Simplifying, these authors represented the process by a two-step kinetic model, previously and independently investigated by Pérez-Benito and coworkers,^{20,22} of random nucleation $A \rightarrow B$ with rate constant k_1 and autocatalytic growth $A + B \rightarrow 2B$ with rate constant k_2 . Analytical solutions $f_{A,FW}(t)$ of the Finke–Watzky kinetic equations¹⁹ are fractions with the time dependence in a fairly complicated denominator:

$$f_{A,FW}(t) = \frac{k_1 + k_2 N_A(0)}{k_2 N_A(0) + k_1 \exp[(k_1 + k_2 N_A(0))t]} \quad (40)$$

which is not simpler to write than our solution $f_A(t) = \exp(Kt_0^4) \exp(-K(t + t_0)^4)$ in **eq 27** for the actual nucleation and growth process in a three-dimensional solid. **Figure 10**

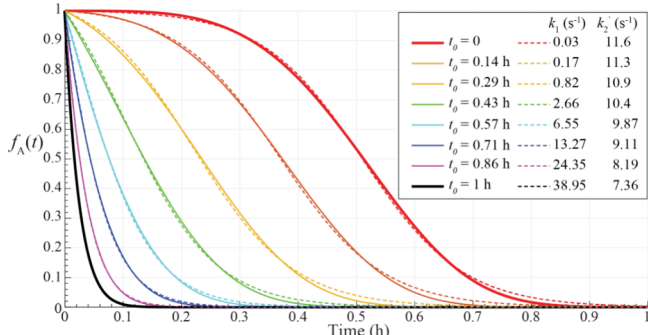


Figure 10. Comparison of (solid lines) conversion $f_A(t) = \exp(Kt_0^4) \exp(-K(t + t_0)^4)$ due to simultaneous nucleation and growth, using $K = 10/h^4$ as in **Figure 6**, with (dashed) best fits by the Finke–Watzky model with the rate-constant parameters k_1 and k_2 as indicated in the legend.

shows the comparison of the Finke–Watzky approximation with our full solution of their nucleation and growth problem for a wide range of parameter values. The Finke–Watzky curves are seen to include a more extended “tail” at long times.

Under the assumption that Avrami and Finke–Watzky theories are “somehow equivalent”,²⁰ Finney and Finke as well as other groups²³ compared fits of experimental data with the Avrami equation and with the Finke–Watzky model. Given that free fitting of either model leads to fairly good agreement with our full solutions for competing nucleation and growth in three-dimensional space, see **Figures 6** and **10**, it is understandable that in most cases both models are nearly equivalent in terms of goodness of fit to experimental data.^{20,23}

Both types of conversion curves in **Figure 10** have two parameters (e.g., K and t_0 in our **eq 27**). Of the two Finke–Watzky parameters, the nucleation rate constant k_1 directly corresponds to the derived parameter

$$k_1 = \dot{n}V_0 = \dot{n}\frac{4}{3}\pi r_0^3 = \frac{4}{3}\pi v^3 n t_0^3 = 4Kt_0^3 \quad (41)$$

of our model, see **eqs 5** and **31**. This is confirmed by the one-to-one relationship between $\dot{n}V_0$ in our model and k_1 of the best Finke–Watzky fits in **Figure 10a**, see **Figure 11a**. Equation

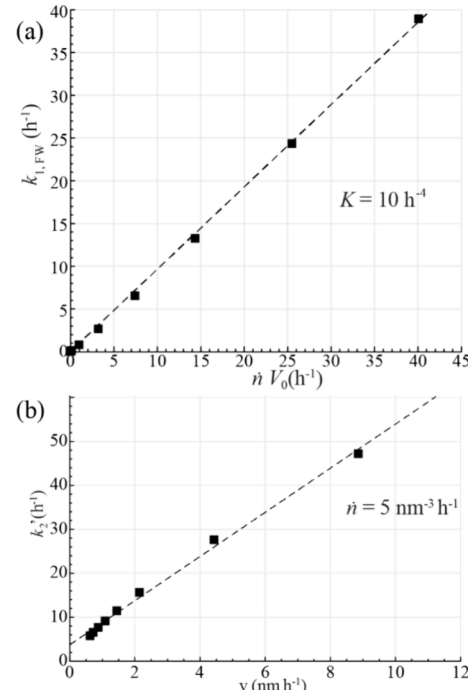


Figure 11. Correlation between (a) the rate constant k_1 in the best-fit Finke–Watzky model curves in **Figure 10** with $k_1 = \dot{n}V_0$ in our full nucleation-and-growth model and (b) the rate constant $k_2' = k_2 N_A(0)$ in the best Finke–Watzky fits with the speed v of the growth front, at constant $V_0 = 1 \text{ nm}^3$ and nucleation rate $\dot{n} = 5 \text{ nm}^{-3} \text{ h}^{-1}$.

41 indicates that (like Avrami K , see **eq 11**, and our $t_0 = r_0/v$) k_1 is not a fundamental physical parameter, since it is the product of the nucleation rate and the initial volume of a nucleus.

Since the representation of particle growth by $A + B \rightarrow 2B$ is simplistic, the rate constant k_2 does not seem to correspond to a specific single parameter of our model. Nevertheless, at a constant nucleation rate \dot{n} , $k_2' = k_2 N_A(0)$ has an approximately linear relation with the growth-front speed v , see **Figure 11b**. Our realistic model avoids the puzzling appearance of initial concentration $[A]_0$ ²⁰ or particle number $N_A(0)$ in expressions like **eq 40**.

4.9. Reparametrization in Terms of Two Rate Constants. Like Finke–Watzky theory, our result of **eq 27** can be written in terms of two rate constants with units of s^{-1} : nucleation-related $k_1 = \dot{n}4/3\pi r_0^3$ as in **eq 41** and growth-related

$$k_0 = 1/t_0 = v/r_0 \quad (42)$$

which again combines a physical rate in space, in this case the rate v of particle growth, with the fundamental length scale r_0 . With **eqs 32** and **42**, we have $K = k_1 k_0^3/4$ and **eq 27** converts to

$$f_A(t) = \exp\left[\frac{1}{4}(k_1/k_0)(1 - (1 + k_0 t)^4)\right] \quad (43)$$

an appealingly simple two-parameter formula for a wide range of sigmoidal curves as shown in Figures 6 and 7. The cooperativity parameter of eq 35 is simply

$$C = \exp(-(k_1/k_0)^{1/4}) \quad (44)$$

5. CONCLUSIONS

We have presented and analyzed an analytical theory for partially cooperative phase conversions, with domain growth in parallel with random conversion, based on the Ishibashi–Takagi modification of standard Avrami theory. It represents an accurate solution of the Finke–Watzky nucleation-and-growth problem in a three-dimensional solid. The amount (fraction) of the initial phase decreases as $f_A(t) = \exp(Kt_0^4) \exp(-K(t + t_0)^4)$ with $K = (\pi/3)v^3n$ from 3D Avrami theory and $V_0 = 4\pi/3v^3t_0^3$ as the initial volume of the nucleus. The prenucleation growth time $t_0 = r_0/v$ relates directly to the linear size r_0 of the critical nucleus or molecular unit and the growth-front speed v . The result $f_A(t)$ can also be expressed in terms of two rate constants, $k_0 = v/r_0$ and Finke–Watzky $k_1 = \dot{n}V_0$. Numerical simulations have confirmed the theory over 4.5 orders of magnitude in nucleation rate. The nucleation rate \dot{n} and growth rate v can sometimes be determined individually, unlike in the conventional Avrami model, where only v^3n can be obtained. Noncooperative exponential first-order kinetics is recovered in the limit of large t_0 . A cooperativity parameter $C = \exp(-\sqrt{2}K^{1/4}t_0)$ can quantify cooperativity between 0 and 1, and it is related to the empirical Avrami exponent n according to $C \approx (n-0.3)/3.7$ for $n \geq 1.45$.

■ AUTHOR INFORMATION

Corresponding Author

Klaus Schmidt-Rohr – Department of Chemistry, Brandeis University, Waltham, Massachusetts 02453, United States;
orcid.org/0000-0002-3188-4828; Email: srohr@brandeis.edu

Authors

Zhenhuan Sun – Department of Chemistry, Brandeis University, Waltham, Massachusetts 02453, United States;
orcid.org/0009-0000-2381-710X

Grace G. D. Han – Department of Chemistry, Brandeis University, Waltham, Massachusetts 02453, United States

Complete contact information is available at:
<https://pubs.acs.org/10.1021/acs.jpcc.4c05750>

Notes

The authors declare no competing financial interest.

■ ACKNOWLEDGMENTS

G.G.D.H. acknowledges the NSF CAREER award (DMR-2142887), Alfred P. Sloan Foundation (FG-2022-18328), and the Camille and Henry Dreyfus Foundation (TC-23-028).

■ REFERENCES

- Kataoka, S.; Kitagawa, D.; Sotome, H.; Ito, S.; Miyasaka, H.; Bardeen, C. J.; Kobatake, S. Relationship between Spatially Heterogeneous Reaction Dynamics and Photochemical Kinetics in Single Crystals of Anthracene Derivatives. *Chem. Sci.* **2024**, *15* (33), 13421–13428.
- Morimoto, K.; Kitagawa, D.; Bardeen, C. J.; Kobatake, S. Cooperative Photochemical Reaction Kinetics in Organic Molecular Crystals. *Chem.—Eur. J.* **2023**, *29* (14), No. e202203291.
- Athiyarath, V.; Mathew, L. A.; Zhao, Y.; Khazeber, R.; Ramamurti, U.; Sureshan, K. M. Rational Design and Topochemical Synthesis of Polymorphs of a Polymer. *Chem. Sci.* **2023**, *14* (19), 5132–5140.
- Krishnan, B. P.; Rai, R.; Asokan, A.; Sureshan, K. M. Crystal-to-Crystal Synthesis of Triazole-Linked Pseudo-Proteins via Topochemical Azide–Alkyne Cycloaddition Reaction. *J. Am. Chem. Soc.* **2016**, *138* (45), 14824–14827.
- Raju, C.; Kunnikuruvan, S.; Sureshan, K. M. Topochemical Cycloaddition Reaction between an Azide and an Internal Alkyne. *Angew. Chem., Int. Ed.* **2022**, *61* (37), No. e202210453.
- Wunderlich, B. *Thermal Analysis of Polymeric Materials*; Springer Science & Business Media, 2005.
- Chakraborty, S.; Nguyen, H. P. Q.; Usuba, J.; Choi, J. Y.; Sun, Z.; Raju, C.; Sigelmann, G.; Qiu, Q.; Cho, S.; Tenney, S. M.; et al. Self-Activated Energy Release Cascade from Anthracene-Based Solid-State Molecular Solar Thermal Energy Storage Systems. *Chem* **2024**, *10*, 3309–3322.
- Avrami, M. Kinetics of Phase Change. I General Theory. *J. Chem. Phys.* **1939**, *7* (12), 1103–1112.
- Avrami, M. Granulation, Phase Change, and Microstructure Kinetics of Phase Change. III. *J. Chem. Phys.* **1941**, *9* (2), 177–184.
- Avrami, M. Kinetics of Phase Change. II Transformation-Time Relations for Random Distribution of Nuclei. *J. Chem. Phys.* **1940**, *8* (2), 212–224.
- Johnson, W. A.; Mehl, R. F. Reaction Kinetics in Processes of Nucleation and Growth. *Trans. Metall. Soc. AIME* **1939**, *135*, 416–442.
- Kolmogorov, A. N. On the Statistical Theory of the Crystallization of Metals. *Bull. Acad. Sci. USSR, Math. Ser.* **1937**, *1*, 335–359.
- Ishibashi, Y.; Takagi, Y. Note on Ferroelectric Domain Switching. *J. Phys. Soc. Jpn.* **1971**, *31* (2), 506–510.
- Gedde, U. *Polymer Physics*; Springer Science & Business Media, 1995.
- Strobl, G. R. *The Physics of Polymers*; Springer, 1997; vol 2.
- Sperling, L. H. *Introduction to Physical Polymer Science*; John Wiley & Sons, 2005.
- Young, R. J.; Lovell, P. A. *Introduction to Polymers*; CRC Press, 2011.
- Tomellini, M.; Fanfoni, M. Why Phantom Nuclei Must be Considered in the Johnson-Mehl-Avrami-Kolmogoroff Kinetics. *Phys. Rev. B* **1997**, *55* (21), 14071–14073.
- Watzky, M. A.; Finke, R. G. Transition Metal Nanocluster Formation Kinetic and Mechanistic Studies. A New Mechanism When Hydrogen Is the Reductant: Slow, Continuous Nucleation and Fast Autocatalytic Surface Growth. *J. Am. Chem. Soc.* **1997**, *119* (43), 10382–10400.
- Finney, E. E.; Finke, R. G. Is There a Minimal Chemical Mechanism Underlying Classical Avrami-Erofe'v Treatments of Phase-Transformation Kinetic Data? *Chem. Mater.* **2009**, *21* (19), 4692–4705.
- Raju, C.; Sun, Z.; Koibuchi, R.; Choi, J. Y.; Chakraborty, S.; Park, J.; Houjou, H.; Schmidt-Rohr, K.; Han, G. G. D. Elucidating the Mechanism of Solid-state Energy Release from Dianthracenes via Auto-catalyzed Cycloreversion. *J. Mater. Chem. A* **2024**, *12* (39), 26678–26686.
- Mata-Pérez, F.; Pérez-Benito, J. Permanganate Ion Oxidation of Amines. *Zeitschrift für Physikalische Chemie* **1984**, *141* (2), 213–219.
- Kearns, E. R.; D'Alessandro, D. M. Variable-Temperature Photocyclization Kinetics in a Metal–Organic Framework (MOF): A Comparison of the Johnson–Mehl–Avrami–Kolmogorov and Finke–Watzky Models. *Cryst. Growth Des.* **2023**, *23* (8), 6100–6106.